

Direct Determination of the Ionization Energies of PtC, PtO, and PtO₂ with VUV Radiation[†]

Murat Citir and Ricardo B. Metz*

Department of Chemistry, University of Massachusetts Amherst, Amherst, Massachusetts 01003

Leonid Belau and Musahid Ahmed

Chemical Sciences Division, Lawrence Berkeley National Laboratory, Berkeley, California 94720

Received: March 20, 2008; Revised Manuscript Received: July 21, 2008

Photoionization efficiency curves were measured for gas-phase PtC, PtO, and PtO₂ using tunable vacuum ultraviolet (VUV) radiation at the Advanced Light Source. The molecules were prepared by laser ablation of a platinum tube, followed by reaction with CH₄ or N₂O and supersonic expansion. These measurements provide the first directly measured ionization energy for PtC, IE(PtC) = 9.45 ± 0.05 eV. The direct measurement also gives greatly improved ionization energies for the platinum oxides, IE(PtO) = 10.0 ± 0.1 eV and IE(PtO₂) = 11.35 ± 0.05 eV. The ionization energy connects the dissociation energies of the neutral and cation, leading to greatly improved 0 K bond dissociation energies for the neutrals: D₀(Pt–C) = 5.95 ± 0.07 eV, D₀(Pt–O) = 4.30 ± 0.12 eV, and D₀(OPt–O) = 4.41 ± 0.13 eV, as well as enthalpies of formation for the gas-phase molecules ΔH⁰_{f,0}(PtC_(g)) = 701 ± 7 kJ/mol, ΔH⁰_{f,0}(PtO_(g)) = 396 ± 12 kJ/mol, and ΔH⁰_{f,0}(PtO_{2(g)}) = 218 ± 11 kJ/mol. Much of the error in previous Knudsen cell measurements of platinum oxide bond dissociation energies is due to the use of thermodynamic second law extrapolations. Third law values calculated using statistical mechanical thermodynamic functions are in much better agreement with values obtained from ionization energies and ion energetics. These experiments demonstrate that laser ablation production with direct VUV ionization measurements is a versatile tool to measure ionization energies and bond dissociation energies for catalytically interesting species such as metal oxides and carbides.

I. Introduction

Transition-metal oxides and carbides have been the subject of numerous experimental and theoretical studies. Much of this interest is due to their relevance to active species in catalytic processes such as the oxidation of CH₄ and CO. Platinum is also extensively used in the petroleum industry as a catalyst for hydrocarbon dehydrogenation, cracking, isomerization, and aromatization. This reformation process produces high-octane gasoline from low-octane feedstock.^{1–5} In the gas phase, neutral platinum atoms react readily with ethane and larger hydrocarbons and can insert into methane, producing H–Pt–CH₃.^{6–8} The Pt⁺ cation is even more reactive, dehydrogenating methane.^{9,10} In addition, several transition-metal oxide cations, including PtO⁺, can directly convert methane to methanol. Schwarz and co-workers^{11,12} describe the Pt⁺-catalyzed oxidation of methane, using oxygen as the oxidant: bare Pt⁺ reacts with methane to form PtCH₂⁺, which then reacts with O₂ to regenerate Pt⁺. Studies of isolated platinum oxides and carbides can aid in revealing the mechanisms and key intermediates of the industrially important reactions. The kinetics and dynamics of the gas-phase reactions can be studied in detail, and the thermodynamics, structure, and spectroscopy of the reaction intermediates can be measured.^{12,13} These molecules are challenging to describe with electronic structure theory due to the number of unpaired electrons and many low-lying electronic states (often having different electron spin states), as well as

the difficulty of accurately treating electron correlation and relativistic effects. Thus, an added motivation for detailed experiments on these small molecules is to provide accurate thermodynamics, structure, and spectroscopy that can be used to evaluate electronic structure methods.

Despite the importance of platinum carbide and oxides, there is little known about their thermodynamics. The only measurements of thermochemical properties of PtC, PtO, and PtO₂ are from high-temperature mass spectrometry/Knudsen cell and transpiration studies. As a recent comprehensive review¹⁴ of these methods points out, they suffer from several potential sources of error, such as sampling errors and uncertainties in ionization cross sections. However, the most serious problem lies in the extrapolations required to obtain 0 K (Kelvin) enthalpies from equilibrium constants measured at ~2000 K. It is thus critical to use a complementary technique to measure bond dissociation energies in these molecules. Extensive guided ion beam studies have measured bond dissociation energies for a wide range of transition-metal-containing ions, with typical uncertainties of 5 kJ/mol.^{15–17} Photodissociation spectra have been measured for some ions, and observed dissociation onsets give an upper limit to the bond dissociation energies.¹⁸ Ionization energies (IE) connect the bond dissociation energies (D₀) of the neutral and ion in a thermodynamic cycle

$$D_0(\text{Pt}–\text{X}) = D_0(\text{Pt}^+–\text{X}) – \text{IE}(\text{Pt}) + \text{IE}(\text{PtX}) \quad (1)$$

As IE(Pt) = 8.9588 eV¹⁹ is precisely known, measuring the ionization energy of the neutral then also determines its bond dissociation energy.

[†] Part of the “Stephen R. Leone Festschrift”.

* To whom correspondence should be addressed. E-mail: rbmetz@chemistry.umass.edu.

The dissociation energy of PtC has been measured in two high-temperature Knudsen cell studies. Vander Auwera-Mahieu and Drowart²⁰ obtained $D_0(\text{Pt}-\text{C}) = 6.30 \pm 0.06$ eV, while Gingerich²¹ derived a value of 6.27 ± 0.11 eV. Zhang and Armentrout have used guided ion beam experiments to measure the 0 K bond dissociation energy of the cation, $D_0(\text{Pt}^+-\text{C}) = 5.46 \pm 0.05$ eV.²² The ionization energy of PtC has not been measured previously, but eq 1 predicts $\text{IE}(\text{PtC}) = 9.80 \pm 0.08$ eV using $D_0(\text{Pt}-\text{C}) = 6.30 \pm 0.06$ eV.

There has only been one determination of the enthalpy of formation of PtO, a high-temperature mass spectrometry/Knudsen cell study by Norman et al.^{23,24} On the basis of measurements from 1750 to 2050 K, a second law enthalpy of formation of $\Delta H_{f,298}^0(\text{PtO}) = 439 \pm 21$ kJ/mol was derived. They also studied PtO₂, obtaining $\Delta H_{f,1900}^0(\text{PtO}_2) = 153 \pm 10$ kJ/mol (they estimate $\Delta H_{f,298}^0(\text{PtO}_2) \approx \Delta H_{f,1900}^0(\text{PtO}_2)$). This implies that bond dissociation energies at 298 K are 3.89 ± 0.22 eV for Pt–O and 5.54 ± 0.24 eV for OPt–O. The Knudsen cell results are in reasonable agreement with earlier, indirect measurements on PtO₂ using the transpiration method by Schäfer and Tebben²⁵ and Alcock and Hooper.²⁶ The thermodynamics of the cations are much better known. In a series of guided ion beam studies, Zhang and Armentrout measured the 0 K bond dissociation energies of the cations, $D_0(\text{Pt}^+-\text{O}) = 3.26 \pm 0.07$ eV and $D_0(\text{OPt}^+-\text{O}) = 3.06 \pm 0.07$ eV.^{22,27,28} The photodissociation spectrum²⁹ of PtO⁺ gives an upper limit to the bond dissociation energy of 3.164 eV, consistent with the ion beam result. Equation 1 then predicts $\text{IE}(\text{PtO}) = 9.59 \pm 0.23$ eV and $\text{IE}(\text{PtO}_2) = 12.03 \pm 0.14$ eV. These values are not consistent with the electron impact ionization energies of 10.1 ± 0.3 eV for PtO and 11.2 ± 0.3 eV for PtO₂ measured by Norman et al.²³ Brönstrup et al.³⁰ observe electron transfer as the major product in the reaction of PtO₂⁺ with C₂H₄ (IE = 10.51 eV), while it is a very minor product with C₂H₂ (IE = 11.40 eV), which implies $\text{IE}(\text{PtO}_2) \leq 11.4$ eV. Direct measurement of the ionization energies of PtC, PtO, and PtO₂ would thus provide accurate thermochemistry for these interesting molecules.

These refractory molecules can only be produced in low concentrations in the gas phase, and one photon ionization requires vacuum ultraviolet (VUV) light at approximately 9.5–11.5 eV. Tunable laboratory VUV sources are often not sufficiently intense to produce the necessary ion signals, while resonant two-color, two-photon ionization ($1 + 1'$ REMPI) is problematic due to the low dissociation energies and high ionization energies of the neutrals. As a result, the experiments are performed using a synchrotron where tunable VUV is readily available.

II. Experimental Approach

These photoionization experiments were carried out at the Chemical Dynamics Beamline at the Advanced Light Source (ALS) at Lawrence Berkeley National Laboratory. The platinum-containing molecules of interest were produced using a pulsed laser ablation source and ionized using tunable vacuum ultraviolet (VUV) light. Experiments were carried out at photon energies of 8–14 eV, with a typical line width of 30 meV. The ALS produces light in pulses separated by only 2 ns; therefore, a high repetition rate ablation source was required to efficiently use this essentially continuous light source. Our previous studies of FeO and CuO used a Nd:YLF ablation laser operating at 1 kHz to ablate rods formed of pressed metal oxide powder.³¹ In the studies reported here, platinum oxides were produced by ablating a rotating/translating platinum tube (Goodfellow, 99.95% pure) synchronously with a pulse of 10% N₂O in He

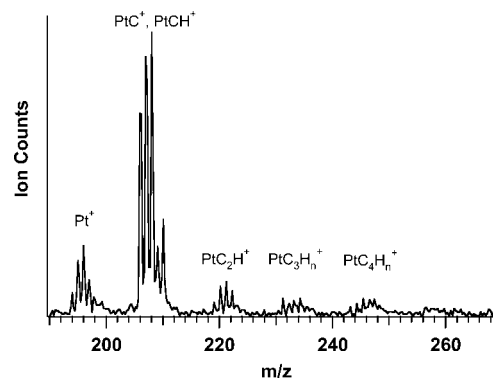


Figure 1. Composite mass spectrum obtained from ablating platinum in methane, showing the production of Pt, PtC, and PtC_xH_y. This is the sum of mass spectra obtained at several photon energies from 11 to 12.8 eV.

from a piezoelectric pulsed valve³² at 2 atm (1 atm = 101.3 KPa) of backing pressure, while PtC was produced using methane, also at 2 atm of backing pressure. The ablation laser was the 532 nm output of a pulsed Nd:YAG laser (Coherent Infinity) operating at 100 Hz repetition rate. Typical pulse energies were 6–10 mJ/pulse, focused to a 80 μm spot with a 35 cm focal length lens. No signal was observed with the Nd:YLF laser, presumably because its longer pulse (160 vs 5 ns) and lower power (4 mJ/pulse) lead to much less ablation.

Ions produced by the source are deflected out of the molecular beam, before the skimmer, by a set of deflection plates. Tunable VUV light crosses the neutral molecular beam 9 cm downstream of the rotating rod, in the extraction region of a reflectron time-of-flight mass spectrometer. Photoions are extracted with a high-voltage pulse and are collected on a microchannel plate detector. Ion time-of-flight spectra are collected with a multichannel scaler card (FAST Comtec 7886). Detailed descriptions of the photoionization spectrometer have been published previously.^{33,34} Our previous studies³¹ of FeO on this instrument show that helium is inefficient at cooling the neutrals, which can lead to photoionization efficiency (PIE) curves that tail to lower energy. As a result, we then used O₂ as the carrier gas, which leads to very sharp onsets, indicating cold ions. To ensure that molecules are thermalized, these studies use 10% N₂O in helium and pure N₂O for PtO and PtO₂, obtaining the same onsets with both gas mixes, and pure CH₄ for PtC. Figure 1 shows a composite mass spectrum obtained by ablating platinum in methane. Platinum has four major isotopes, ¹⁹⁴Pt (33%), ¹⁹⁵Pt (34%), ¹⁹⁶Pt (25%), and ¹⁹⁸Pt (7%). The intensities of the mass peaks in the 206–210 amu range differ slightly from those predicted from the isotopic abundances, indicating that, in addition to PtC, the source produces small amounts of PtCH and PtCH₂. The source also produces PtC₂H_x and PtC₃H_x, and results on the larger compounds will be presented separately. Photoionization efficiency curves are measured by integrating the signal from PtC, PtO, and PtO₂ as a function of VUV energy and normalizing to photon flux. To avoid interference from PtCH, only the signal for ¹⁹⁴PtC ($m/z = 206$) is integrated. For the oxides, the PIE curves are summed over the major isotopes.

III. Results and Discussion

A. Photoionization of PtC. A survey of photoionization efficiency (PIE) spectrum of PtC from 8 to 14 eV is shown in Figure 2a. Figure 2b shows the results of additional scans taken with a smaller (100 meV) step size. The photoionization onset is sharp and occurs at 9.45 ± 0.05 eV. The same onset is

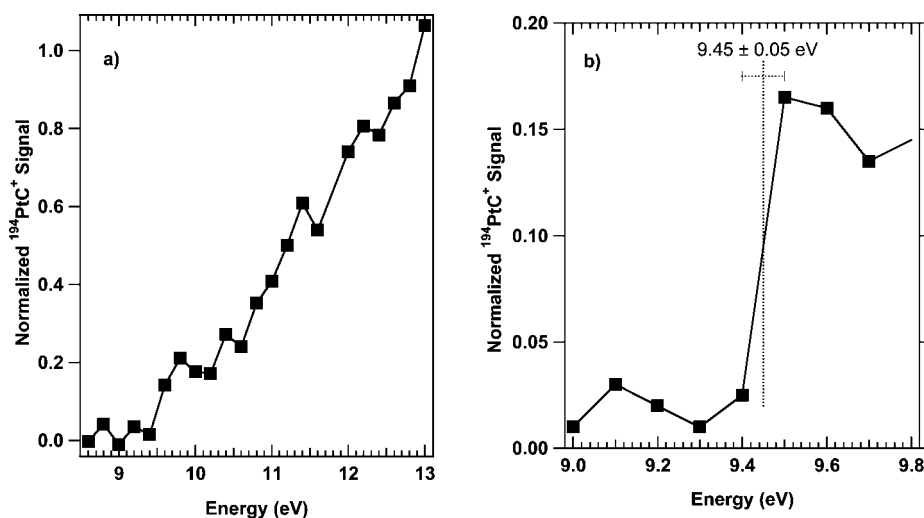


Figure 2. Photoionization efficiency curves for ^{194}PtC ; (a) survey spectrum with data points separated by 200 meV and (b) region near the ionization onset with data points every 100 meV. The vertical line and error bars indicate the ionization energy of 9.45 ± 0.05 eV.

TABLE 1: Experimental Ionization Energies, Enthalpies of Formation, and Bond Dissociation Energies of PtC, PtO, and PtO₂

	IE (eV)	$\Delta H_{f,0}^0$ (kJ/mol)	D_0 (eV) ^a
PtC	9.45 ± 0.05^b	701 ± 7^c	5.95 ± 0.07^c
			6.30 ± 0.06^d
			6.27 ± 0.11^e
PtO	10.0 ± 0.1^b	396 ± 12^c	4.30 ± 0.12^c
	10.1 ± 0.3^f	439 ± 21^g	3.89 ± 0.22^g
			3.94 ± 0.22^h
PtO ₂	11.35 ± 0.05^b	218 ± 11^c	4.41 ± 0.13^c
	11.2 ± 0.3^f	153 ± 10^i	5.54 ± 0.24^g
		173^j	4.88 ± 0.24^h
		164.4 ± 1.3^k	
		212 ± 11^h	

^a For PtO₂, $D_0(\text{OPt}-\text{O})$. ^b This work. ^c This work and eq 1; ion energetics from refs 22, 27, and 28 and $\Delta H_{f,0}^0(\text{Pt}_{(g)})$ from ref 36. ^d Knudsen cell.²⁰ ^e Knudsen cell.²¹ ^f Electron impact.²³ ^g Second law value from Knudsen cell measurement, 298 K value.^{23,24} ^h Third law value, this work, from Knudsen cell data.²³ ⁱ Second law value from Knudsen cell measurements,^{23,24} assumed independent of temperature. ^j Second law value from transpiration study,²⁵ 298 K value. ^k Second law value from transpiration study,²⁶ 1600 K value.

obtained from data taken at 50 meV intervals. Zhang and Armentrout have used guided ion beam experiments to measure the 0 K bond dissociation energy of the cation, $D_0(\text{Pt}^+-\text{C}) = 5.46 \pm 0.05$ eV.²² Combining this value with IE(Pt) = 8.9588 eV and using eq 1 gives the 0 K dissociation energy of the neutral, $D_0(\text{Pt}-\text{C}) = 5.95 \pm 0.07$ eV. Subtracting this value from the enthalpies of formation of atomic carbon³⁵ (711.2 kJ/mol) and platinum³⁶ (564 ± 2 kJ/mol) gives the enthalpy of formation $\Delta H_{f,0}^0(\text{PtC}_{(g)}) = 701 \pm 7$ kJ/mol (Table 1). The dissociation energy of PtC has been measured in two high-temperature Knudsen cell studies. Vander Auwera-Mahieu and Drowart measured the ratio of PtC⁺/Pt⁺ (produced by electron impact) as a function of temperature from 2150 to 2450 K. They then obtained $D_0(\text{Pt}-\text{C}) = 6.30 \pm 0.06$ eV using the second and third law methods.²⁰ A later study by Gingerich²¹ on ThPt and ThIr found discrepancies with dissociation energies of PtC and IrC measured by Drowart and co-workers. He remeasured $D_0(\text{Pt}-\text{C})$ and obtained 6.27 ± 0.11 eV. The discrepancy with our values, while outside of the combined uncertainties, is not large, particularly considering the potential error introduced by extrapolation to 0 K. They used the thermodynamic functions

for graphite and Pt_(s) and derived values for PtC_(g) based on the ground-state spectroscopic parameters.

In order to determine reasons for the discrepancy, and larger discrepancies observed for the platinum oxides, the Knudsen cell experiments were examined in more detail. Two potential sources of error¹⁴ in the interpretation of the Knudsen cell data are the assumption that electron impact ionization cross sections of Pt and PtC are the same and possible errors in the thermodynamic functions for PtC. Scott and Irikura have shown that, for a wide variety of molecules, the binary-encounter Bethe (BEB) method³⁷ correctly predicts the magnitude and shape of the cross section, even at energies only a few eV above the ionization energy.^{38,39} BEB cross sections for Pt and PtC are calculated here following the procedure of Scott and Irikura. Calculations are carried out with the Hartree-Fock method and the 6-311+G(d) basis on carbon and SDD basis and relativistic effective core potential for platinum using Gaussian03. Kinetic energies of orbitals are calculated using the (iop 6/81 = 3) keyword, and orbital ionization energies are calculated with the outer-valence Green's function (OVGF) method. Experimental ionization energies are used where possible. At the 75 eV electron energy used in the experiment of Vander Auwera-Mahieu and Drowart, the calculated cross sections are identical, 7.40 Å² for Pt and 7.39 Å² for PtC.

The spectroscopy of PtC has been studied extensively. High-temperature absorption and emission studies^{40–42} determined the ground state to be ${}^1\Sigma^+$, with $\omega_e = 1051.1$ cm⁻¹ and $\omega_e x_e = 4.86$ cm⁻¹. Vander Auwera-Mahieu and Drowart calculated thermodynamic functions for PtC based on a harmonic ${}^1\Sigma^+$ ground state with $\omega_e = 1051.1$ cm⁻¹. Molecular beam high-resolution laser-induced fluorescence and Stark spectroscopy studies by Steimle and co-workers^{43–45} show that PtC (X, ${}^1\Sigma^+$) has a bond length of $r_e = 1.679$ Å and a dipole moment of only 1.09 D. Including vibrational anharmonicity and excited electronic states has a negligible effect on the thermodynamic functions for PtC, even at 2300 K, as the lowest excited state of PtC is at $\sim 12,700$ cm⁻¹. Statistical mechanical thermodynamic functions⁴⁶ for PtC are given in Table S1 (Supporting Information). This analysis suggests that the discrepancy in $D_0(\text{Pt}-\text{C})$ between our results and the Knudsen cell results is not due to incorrect assumptions about the electron impact ionization cross sections of Pt and PtC or to the use of incomplete thermodynamic functions; rather, this discrepancy

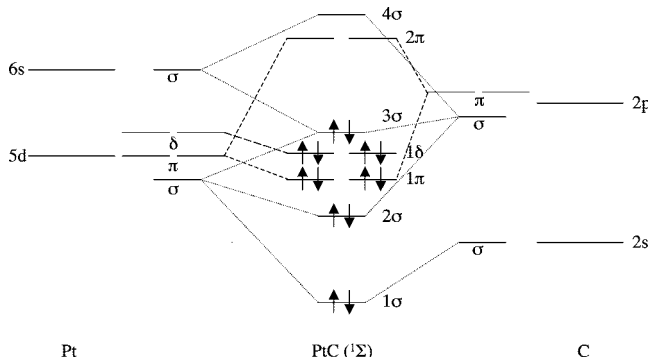


Figure 3. Schematic molecular orbital correlation diagram and electron occupancy for PtC (X, $^1\Sigma$).

could arise from other factors in the Knudsen cell experiment, such as sampling discrimination.

The first ab initio calculations on PtC were performed by Minaev, who used multireference configuration interaction (MRCI), including spin-orbit coupling, to characterize the excited electronic states responsible for the observed transitions in the visible and near-ultraviolet.⁴⁷ The states responsible for the red bands, which were previously thought to be $^1\Pi$ and $^1\Sigma$ states, were reassigned as the $\Omega = 1$ and 0^+ sublevels of a $^3\Pi$ state. The calculated bond length and dipole moment for the ground state are in good accord with experiment.^{43–45} A schematic molecular orbital diagram for PtC, based on the one presented by Minaev, is shown in Figure 3. Minaev finds that the ground state is well described (83%) by the configuration $1\sigma^2 2\sigma^2 1\pi^4 2\pi^4 1\delta^4 3\sigma^2$. The $^3\Pi_{0,1}$ states, formed by a $3\sigma \rightarrow 2\pi$ excitation,⁴⁷ have a dipole moment of 1.9 D, significantly larger than that of the ground state (1.09 D).⁴⁵ This indicates that the 2π is a carbon-centered, antibonding orbital. The other recent calculation, by Wang et al., used the B3LYP hybrid density functional method to calculate spectroscopic parameters, bond dissociation energies, and ionization energies of the neutrals, cations, and anions of the third-row transition-metal carbides.⁴⁸ For PtC, they predict a $^1\Sigma^+$ ground state with $r_e = 1.683 \text{ \AA}$, $\omega_e = 1097 \text{ cm}^{-1}$, and a dissociation energy of $D_e = 5.93 \text{ eV}$ ($D_0 = 5.86 \text{ eV}$). The cation is very similar, with $r_e = 1.676 \text{ \AA}$, $\omega_e = 1073 \text{ cm}^{-1}$, and $D_e = 5.88 \text{ eV}$ ($D_0 = 5.81 \text{ eV}$). The ground state of PtC⁺ is $^2\Sigma$, corresponding to the removal of an electron from the nonbonding 3σ orbital of PtC. The calculated ionization energy is 9.39 eV, which agrees very well with our result of $9.45 \pm 0.05 \text{ eV}$. This agreement is largely fortuitous; the calculations overestimate IE(Pt) and $D_0(\text{Pt}^+ - \text{C})$ by $\sim 0.35 \text{ eV}$, and the errors cancel. The calculations show that there is little geometry change upon ionization, and this is confirmed in our work by the sharp photoionization onset.

B. Photoionization of PtO and PtO₂. Figures 4 and 5 show photoionization efficiency curves for PtO and PtO₂. The ionization onset of PtO₂ is sharp and occurs at $11.35 \pm 0.05 \text{ eV}$, while that of PtO is not as distinct and occurs at $10.0 \pm 0.1 \text{ eV}$. The same onsets are obtained from data taken at 50 meV intervals and using pure N₂O as the reactant rather than 10% N₂O in He. These values confirm and refine the ionization energies of $10.1 \pm 0.3 \text{ eV}$ for PtO and $11.2 \pm 0.3 \text{ eV}$ for PtO₂ measured by Norman et al. using electron impact.²³ Also, the 11.35 eV ionization energy for PtO₂ is consistent with the observation in the ion cyclotron resonance spectrometer reaction study³⁰ of electron transfer as the major product in the reaction of PtO₂⁺ with C₂H₄ (IE = 10.51 eV) and as a very minor product with C₂H₂ (IE = 11.40 eV).

The measured ionization energies of PtO and PtO₂ allow the determination of the neutral bond dissociation energies from

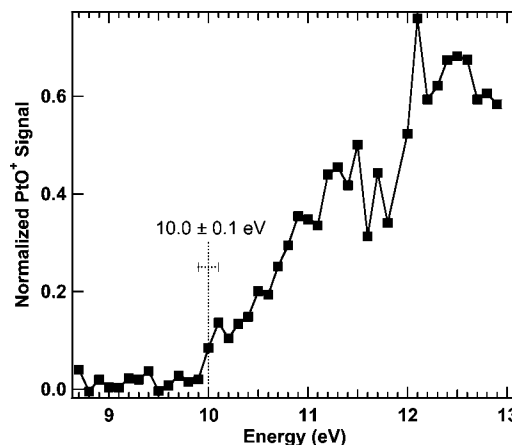


Figure 4. Photoionization efficiency curve of PtO. Data points are separated by 100 meV, and the vertical line and error bars indicate the ionization energy of $10.0 \pm 0.1 \text{ eV}$.

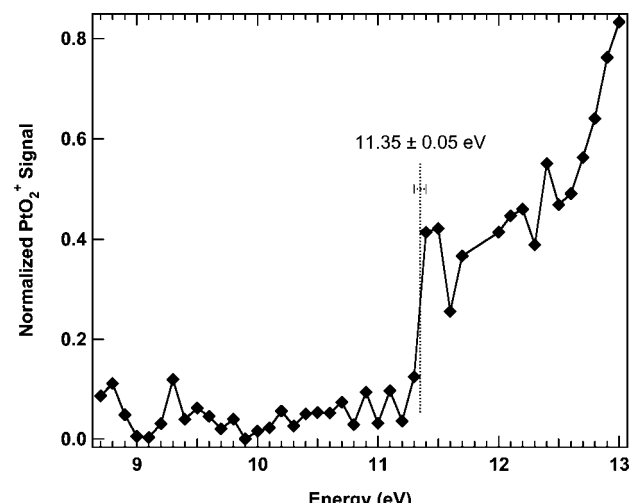
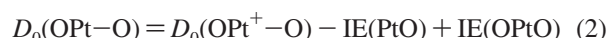


Figure 5. Photoionization efficiency curve of PtO₂. The vertical line and error bars indicate the ionization energy of $11.35 \pm 0.05 \text{ eV}$. Data points are separated by 100 meV.

those of the ions using a thermodynamic cycle (eq 1). Zhang and Armentrout measured the 0 K bond dissociation energies of the cations $D_0(\text{Pt}^+ - \text{O}) = 3.26 \pm 0.07 \text{ eV}$ and $D_0(\text{OPt}^+ - \text{O}) = 3.06 \pm 0.07 \text{ eV}$ from several endothermic ion-molecule reactions in a guided ion beam apparatus.^{22,27,28} The value for PtO⁺ is consistent with the upper limit of 3.164 eV from the photodissociation onset.²⁹ The resulting bond dissociation energy $D_0(\text{Pt} - \text{O})$ is $4.30 \pm 0.12 \text{ eV}$. For PtO₂, the analogue of eq 1 is



and $D_0(\text{OPt} - \text{O}) = 4.41 \pm 0.13 \text{ eV}$, at 0 K. The Knudsen cell measurements^{23,24} give second law bond dissociation energies at 298 K of $3.89 \pm 0.22 \text{ eV}$ for Pt-O and $5.54 \pm 0.24 \text{ eV}$ for O⁺Pt-O. The value for Pt-O is low, while that for O⁺Pt-O is clearly too high, suggesting possible errors in the measurement or analysis. This will be explored in more detail below. A more direct comparison with the high-temperature studies of PtO₂ can be obtained by using the guided ion beam results for the enthalpy for the insertion of Pt⁺ into O₂



From the ionization energies of PtO₂ and Pt, one obtains ΔH (0 K) = $-3.59 \pm 0.11 \text{ eV}$ ($-346 \pm 11 \text{ kJ/mol}$) for the

corresponding neutral reaction. Adding the enthalpy of vaporization of platinum, $\Delta H_{f,0}^0(\text{Pt}_{(g)}) = 564 \pm 2 \text{ kJ/mol}$ ³⁶ gives the enthalpy of formation of PtO₂



Knudsen cell measurements from 1750 to 2050 K by Norman et al.^{23,24} give a second law value of $\Delta H_{f,1900}^0(\text{PtO}_2) = 153 \pm 10 \text{ kJ/mol}$; they assume that this value is independent of temperature. In earlier indirect measurements using the transpiration method, Schäfer and Tebben obtained $\Delta H_{f,1430}^0(\text{PtO}_2) = 168 \text{ kJ/mol}$ and estimated $\Delta H_{f,298}^0(\text{PtO}_2) = 173 \text{ kJ/mol}$ from measurements from 1380 to 1481 K,²⁵ while Alcock and Hooper got $\Delta H_{f,1600}^0(\text{PtO}_2) = 164.4 \pm 1.3 \text{ kJ/mol}$ from measurements from 1370 to 1820 K.²⁶ These values are all somewhat lower than the 0 K value obtained here using the ionization energy and ion thermochemistry (see Table 1). As with PtC, we will assess how electron impact cross sections and thermodynamic functions affect the analysis of the high-temperature mass spectrometry studies.

Norman et al.²³ assumed that ionization cross sections for the platinum oxides are additive, giving relative cross sections of 1/1.107/1.214 for Pt/PtO/PtO₂. Because electron impact ionization cross sections are a major potential source of inaccuracy, they were examined in detail in a critical assessment of high-temperature mass spectrometry measurements. Measurements for several metal oxides show that the cross sections are not additive and that monoxides typically have $\sim 35\%$ smaller cross sections than the metal, and those of the dioxide are smaller still.¹⁴ Our calculated (BEB) relative cross sections at the electron energies used by Norman et al. are 1/0.66/0.86 for Pt/PtO/PtO₂. The relatively large cross section for PtO₂ is due to the presence of several low-lying orbitals from which an electron can be removed. The revised cross sections increase $D_0(\text{Pt}-\text{O})$ by 0.14 eV and decrease $D_0(\text{OPt}-\text{O})$ by 0.03 eV.

As there was no spectroscopic information available at the time of Norman et al.'s experiment, they used generic metal oxide thermodynamic functions for PtO and did not include any temperature corrections for PtO₂. Since then, there have been numerous spectroscopic investigations of PtO and PtO₂. Several emission studies have explored the rich electronic spectrum of PtO.^{49–52} The absorption spectrum of PtO in a rare gas matrix has been measured to characterize its electronic⁵³ and vibrational^{54,55} states. Photoelectron spectroscopy of PtO[−] reveals additional low-lying states of PtO.⁵⁶ The ground state of PtO is the $\Omega = 0^+$ component (in Hund's case (c)) of a ${}^3\Sigma^-$ state; the $\Omega = 1$ component lies 946 cm^{-1} higher in energy. The ground state has $\omega_e = 851.07 \text{ cm}^{-1}$ and $\omega_ex_e = 4.96 \text{ cm}^{-1}$ and a dipole moment of 2.77 D.^{43,51} Recently, Cooke and Gerry⁵⁷ and Okabayashi et al.⁵⁸ have measured the microwave spectrum of PtO. The rotational constants gave a bond length of $r_e = 1.727 \text{ \AA}$ for PtO. The most detailed spectroscopic studies of PtO₂ are the matrix isolation infrared absorption work by Andrews and co-workers.^{54,55,59} They obtained spectra for OPtO and Pt(O₂) with ¹⁶O and ¹⁸O. For ¹⁶OPt¹⁶O, they observed the bend $\nu_2 = 157 \text{ cm}^{-1}$ and antisymmetric stretch $\nu_3 = 953 \text{ cm}^{-1}$. They did not observe the symmetric stretch ν_1 , but the $\nu_1 + \nu_3$ combination band was at 1838 cm^{-1} . They did, however observe ν_1 at 861 cm^{-1} for the mixed isotopomer ¹⁶OPt¹⁸O. This strongly suggests that OPtO is linear, in accord with their B3LYP calculations, which predict a ${}^1\Sigma_g^+$ ground state. The photoelectron spectrum of OPtO[−] shows a single long progression at $895 \pm 30 \text{ cm}^{-1}$, which has been assigned to the symmetric stretch.⁵⁶ These spectroscopic parameters were used to calculate the

statistical mechanical thermodynamic functions for PtO and PtO₂. Statistical mechanical thermodynamic functions⁴⁶ for PtO and PtO₂ are given in Table S1 (Supporting Information). This, along with the tabulated values³⁶ for Pt_(s), is used to calculate third law dissociation energies from the experimental measurements by Norman et al. at 2018 K. The most dramatic changes involve PtO₂. Norman et al. obtained $\Delta H_{f,1900}^0(\text{PtO}_{2(g)}) = 153 \pm 10 \text{ kJ/mol}$ (the temperature dependence was assumed to be small) and an apparent ΔS from the second law calculation of $-21 \pm 5 \text{ J/(mol K)}$. In contrast, the statistical mechanical calculation performed here gives $\Delta S_{f,2018}^0(\text{PtO}_{2(g)}) = 5.2 \text{ J/(mol K)}$. As a result, the revised, third law value is $\Delta H_{f,0}^0(\text{PtO}_{2(g)}) = 212 \text{ kJ/mol}$, which is in excellent agreement with the value ($218 \pm 11 \text{ kJ/mol}$) obtained from the ion energetics and ionization energy of PtO₂. The PtO₂ pressures measured in the transpiration studies^{25,26} appear to be too high by a factor of ~ 40 , which was also noted by Norman et al.^{23,24} The 0 K third law bond dissociation energies from the Knudsen cell measurements are $D_0(\text{Pt}-\text{O}) = 3.94 \pm 0.22 \text{ eV}$ and $D_0(\text{OPt}-\text{O}) = 4.88 \pm 0.24 \text{ eV}$. For comparison, the original second law values are $3.89 \pm 0.22 \text{ eV}$ for Pt-O and $5.54 \pm 0.24 \text{ eV}$ for OPt-O. The third law values are in reasonable agreement with the bond dissociation energies obtained from our measured ionization energies and the ion energetics, $D_0(\text{Pt}-\text{O}) = 4.30 \pm 0.12 \text{ eV}$ and $D_0(\text{OPt}-\text{O}) = 4.41 \pm 0.13 \text{ eV}$.

Calculations show that the molecular orbital scheme outlined for PtC in Figure 3 also applies to PtO. Heinemann et al.⁶⁰ carried out complete active-space self-consistent field (CAS-SCF) calculations on PtO and PtO⁺, including spin-orbit effects via a one-electron spin-orbit operator. They predicted that the ground state of PtO is the $\Omega = 0$ component of a ${}^3\Sigma^-$ state, with the electron configuration $1\sigma^2 2\sigma^1 1\pi^4 1\delta^4 3\sigma^2 2\pi^2$, in accord with experiment. In going from PtC to PtO, the measured bond length increases from 1.679 to 1.727 Å, while the vibrational frequency decreases from 1051 to 851 cm^{−1}, and the bond dissociation energy drops from 5.95 to 4.30 eV, all consistent with the 2π orbital being weakly antibonding. The dipole moment increases from 1.09 to 2.77 D, indicating that the 2π orbital is primarily oxygen-centered.

The CAS-SCF calculations predict $r_e = 1.792 \text{ \AA}$ and $\omega_e = 719 \text{ cm}^{-1}$, and the discrepancy with experiment is consistent with the lack of dynamic electron correlation in the calculation. Cooke and Gerry⁵⁷ also carried out density functional theory calculations on PtO, approximately accounting for relativistic effects using the zero-order regular approximation (ZORA) and statistical average of orbital potentials (SAOP) methods. They obtained $r_e = 1.7253 \text{ \AA}$, $\omega_e = 907.6 \text{ cm}^{-1}$, $\omega_ex_e = 8.17 \text{ cm}^{-1}$, and $D_e = 5.38 \text{ eV}$ ($D_0 = 5.32 \text{ eV}$). Although the bond length is in excellent agreement with experiment, the vibrational frequency and bond dissociation energy are too high. The ground state of PtO⁺ is produced by removing an electron from the 3σ orbital, leading to a ${}^4\Sigma^-$ state with a calculated⁶⁰ bond length of $r_e = 1.815 \text{ \AA}$. The $\Omega = 1/2$ component is predicted to lie 0.05 eV above $\Omega = 3/2$. A ${}^4\Sigma_{-3/2}$ ground state is consistent with rotational structure in the photodissociation spectrum of jet-cooled PtO⁺ measured by Thompson et al.,²⁹ who observed transitions from the $\Omega = 3/2$ component but not from $\Omega = 1/2$. Unfortunately, the bond length of PtO⁺ could not be determined as the predissociation lifetime²⁹ resulted in linewidths of $> 1 \text{ cm}^{-1}$. The similarity in bond length between PtO and PtO⁺ would lead one to expect a sharp photoionization onset. The observed onset is broader than that of PtC or PtO₂. This could be due to unresolved, overlapping transitions to the $\Omega = 3/2$ and $1/2$ components of the ${}^4\Sigma^-$ state of PtO⁺. Simple

density functional calculations of IE(PtO) give a wide range of values, from 9.87 (BLYP) to 11.35 eV (B3P86); the B3LYP value of 10.71 eV is 0.7 eV too high.⁶¹

Brönstrup et al.³⁰ carried out a series of calculations assessing the relative stabilities of O⁺PtO and its isomer PtOO⁺. Calculations at the B3LYP level with a modest basis set predict that PtOO⁺ is more stable by ~1 eV; B3LYP calculations with larger basis sets predict that they are essentially isoenergetic. Upon performing much more demanding multireference second-order perturbation theory calculations, O⁺PtO is more stable by ~1 eV. The authors note that this should serve as a warning that the popular B3LYP method can substantially underestimate bond dissociation energies for some systems (such as O⁺PtO), while it is quite reliable for related molecules such as PtO⁺ and PtOO⁺. As part of their matrix isolation IR study, Bare et al. carried out B3LYP calculations on O⁺PtO and PtOO.⁵⁴ They found that O⁺PtO is linear, with a ${}^1\Sigma_g^+$ ground state, consistent with their infrared spectra. The B3LYP calculations predict that the O⁺PtO isomer is 1.50 eV more stable than PtOO. However, they substantially underestimate the stability of O⁺PtO, as the calculated exothermicity for Pt + O₂ → O⁺PtO is 2.38 eV, which is 1.21 eV too low. Therefore, the O⁺PtO isomer is likely to be ~2.7 eV more stable than PtOO. The caution raised by Brönstrup et al. with respect to O⁺PtO appears to also apply to the neutral; B3LYP calculations can give erroneous bond dissociation energies for some systems, while they are quite accurate for (apparently) similar molecules. This highlights the necessity for accurate thermochemistry for these metal-containing molecules. Accurate bond dissociation energies of the neutrals can be obtained from ionization energies and ion bond dissociation energies. Older values based on high-temperature mass spectrometry can have large errors, especially if they are based solely on a second law analysis.

IV. Conclusions

A laser ablation source, coupled with direct VUV ionization, is a versatile technique to measure ionization energies for coordinatively unsaturated transition metal-oxides and carbides. In conjunction with bond dissociation energies for the corresponding ions, the ionization energies give bond dissociation energies for the neutrals which are more accurate and precise than those obtained using high-temperature Knudsen cell mass spectrometry. Third law calculations using Knudsen cell data of the enthalpies of formation of PtO₂ and bond dissociation energies of PtO and O⁺Pt–O lead to greatly improved values compared to the original second law calculations.

Acknowledgment. R.B.M. acknowledges financial support from the National Science Foundation under Award CHE-0608446. This work was supported by the Director, Office of Energy Research, Office of Basic Energy Sciences, Chemical Sciences Division of the U.S. Department of Energy under Contract No. DE-AC02-05CH11231.

Supporting Information Available: Table S1. Shomate equation coefficients for statistical thermodynamic functions for PtC, PtO, and PtO₂. This material is available free of charge via the Internet at <http://pubs.acs.org>.

References and Notes

- Centi, G.; Cavani, F.; Trifirò, F. *Selective Oxidation by Heterogeneous Catalysis*; Kluwer Academic: New York, 2001.
- Metal-Oxo and Metal-Peroxo Species in Catalytic Oxidations*; Meunier, B., Ed.; Springer-Verlag: Berlin, Germany, 2000; Vol. 97.
- Shilov, A. E.; Shtainman, A. A. *Acc. Chem. Res.* **1999**, 32, 763.
- Somorjai, G. A. *Introduction to Surface Science and Catalysis*; Wiley: New York, 1994.
- Crabtree, R. H. *The Organometallic Chemistry of the Transition Metals*, 4th ed.; Wiley: New York, 2005.
- Carroll, J. J.; Weisshaar, J. C. *J. Phys. Chem.* **1996**, 100, 12355.
- Carroll, J. J.; Weisshaar, J. C.; Siegbahn, P. E. M.; Wittborn, C. A. M.; Blomberg, M. R. A. *J. Phys. Chem.* **1995**, 99, 14388.
- Campbell, M. L. *J. Chem. Soc., Faraday Trans.* **1998**, 94, 353.
- Irikura, K. K.; Beauchamp, J. L. *J. Phys. Chem.* **1991**, 95, 8344.
- Irikura, K. K.; Goddard, W. A., III. *J. Am. Chem. Soc.* **1994**, 116, 8733.
- Pavlov, M.; Blomberg, M. R. A.; Siegbahn, P. E. M.; Wesendrup, R.; Heinemann, C.; Schwarz, H. *J. Phys. Chem. A* **1997**, 101, 1567.
- Böhme, D. K.; Schwarz, H. *Angew. Chem., Int. Ed.* **2005**, 44, 2336.
- Metz, R. B. *Adv. Chem. Phys.* **2008**, 138, 331.
- Drowart, J.; Chatillon, C.; Hastie, J.; Bonnell, D. *Pure Appl. Chem.* **2005**, 77, 683.
- Armentrout, P. B.; Kickel, B. L. Gas-Phase Thermochemistry of Transition Metal Ligand Systems: Reassessment of Values and Periodic Trends. In *Organometallic Ion Chemistry*; Freiser, B. S., Ed.; Kluwer Academic Publishers: Dordrecht, The Netherlands, 1994; p 1.
- Armentrout, P. B. *Int. J. Mass Spectrom.* **2000**, 200, 219.
- Armentrout, P. B. *Int. J. Mass Spectrom.* **2003**, 227, 289.
- Metz, R. B. *Int. Rev. Phys. Chem.* **2004**, 23, 79.
- Jakubek, Z. J.; Simard, B. *J. Phys. B* **2000**, 33, 1827.
- Vander Auwera-Mahieu, A. V.; Drowart, J. *Chem. Phys. Lett.* **1967**, 1, 311.
- Gingerich, K. A. *Chem. Phys. Lett.* **1973**, 23, 270.
- Zhang, X. G.; Armentrout, P. B. *J. Phys. Chem. A* **2003**, 107, 8904.
- Norman, J. H.; Staley, H. G.; Bell, W. E. *J. Phys. Chem.* **1967**, 71, 3686.
- Norman, J. H.; Staley, H. G.; Bell, W. E. *Adv. Chem. Ser.* **1968**, 72, 101.
- Schäfer, H.; Tebben, A. Z. *Anorg. Allg. Chem.* **1960**, 304, 317.
- Alcock, C. B.; Hooper, G. W. *Proc. R. Soc. London, Ser. A* **1960**, 254, 551.
- Zhang, X. G.; Armentrout, P. B. *J. Phys. Chem. A* **2003**, 107, 8915.
- Zhang, X. G.; Armentrout, P. B. *Eur. J. Mass Spectrom.* **2004**, 10, 963.
- Thompson, C. J.; Stringer, K. L.; McWilliams, M.; Metz, R. B. *Chem. Phys. Lett.* **2003**, 376, 588.
- Brönstrup, M.; Schröder, D.; Kretzschmar, I.; Schwarz, H.; N. Harvey, J. *J. Am. Chem. Soc.* **2001**, 123, 142.
- Metz, R. B.; Nicolas, C.; Ahmed, M.; Leone, S. R. *J. Chem. Phys.* **2005**, 123, 114313.
- Proch, D.; Trickl, T. *Rev. Sci. Instrum.* **1989**, 60, 713.
- Nicolas, C.; Shu, J.; Peterka, D. S.; Poisson, L.; Leone, S. R.; Ahmed, M. *J. Am. Chem. Soc.* **2006**, 128, 220.
- Belau, L.; Wheeler, S. E.; Ticknor, B. W.; Ahmed, M.; Leone, S. R.; Allen, W. D.; Schaefer, H. F., III; Duncan, M. A. *J. Am. Chem. Soc.* **2007**, 129, 10229.
- Chase, M. W., Jr. *J. Phys. Chem. Ref. Data* **1998**, Monograph 9, 1.
- Arblaster, J. W. *Platinum Met. Rev.* **2005**, 49, 141.
- Hwang, W.; Kim, Y. K.; Rudd, M. E. *J. Chem. Phys.* **1996**, 104, 2956.
- Huo, W. M.; Kim, Y. K. *Chem. Phys. Lett.* **2000**, 319, 576.
- Scott, G. E.; Irikura, K. K. *J. Chem. Theory Comput.* **2005**, 1, 1153.
- Scullman, R.; Yttermo, B. *Ark. Fys.* **1966**, 33, 231.
- Appelblad, O.; Barrow, R. F.; Scullman, R. *Proc. Phys. Soc., London* **1967**, 91, 260.
- Appelblad, O.; Nilsson, C.; Scullman, R. *Phys. Scr.* **1973**, 7, 65.
- Steimle, T. C.; Jung, K. Y.; Li, B. Z. *J. Chem. Phys.* **1995**, 103, 1767.
- Steimle, T. C.; Jung, K. Y.; Li, B. Z. *J. Chem. Phys.* **1995**, 102, 5937.
- Beaton, S. A.; Steimle, T. C. *J. Chem. Phys.* **1999**, 111, 10876.
- Irikura, K. K. Essential Statistical Thermodynamics. In *Computational Thermochemistry: Prediction and Estimation of Molecular Thermodynamics*; Irikura, K. K., Frurip, D. J., Eds.; ACS Symposium Series 677; American Chemical Society: Washington, DC, 1998; App. B.
- Minaev, B. F. *Phys. Chem. Chem. Phys.* **2000**, 2, 2851.
- Wang, J. P.; Sun, X. B.; Wu, Z. J. *Cluster Sci.* **2007**, 18, 333.
- Nilsson, C.; Scullman, R.; Mehendale, N. *J. Mol. Spectrosc.* **1970**, 35, 177.
- Scullman, R.; Sassenberg, U.; Nilsson, C. *Can. J. Phys.* **1975**, 53, 1991.
- Sassenberg, U.; Scullman, R. *Phys. Scr.* **1983**, 28, 139.
- Frum, C. I.; Engleman, R.; Bernath, P. F. *J. Mol. Spectrosc.* **1991**, 150, 566.
- Jansson, K.; Scullman, R. *J. Mol. Spectrosc.* **1976**, 61, 299.
- Bare, W. D.; Citra, A.; Chertihin, G. V.; Andrews, L. *J. Phys. Chem. A* **1999**, 103, 5456.

- (55) Wang, X. F.; Andrews, L. *J. Phys. Chem. A* **2001**, *105*, 5812.
(56) Ramond, T. M.; Davico, G. E.; Hellberg, F.; Svedberg, F.; Salen, P.; Soderqvist, P.; Lineberger, W. C. *J. Mol. Spectrosc.* **2002**, *216*, 1.
(57) Cooke, S. A.; Gerry, M. C. L. *Phys. Chem. Chem. Phys.* **2005**, *7*, 2453.
(58) Okabayashi, T.; Yamazaki, E.; Tanimoto, M. *J. Mol. Spectrosc.* **2005**, *229*, 283.
(59) Danset, D.; Manceron, L.; Andrews, L. *J. Phys. Chem. A* **2001**, *105*, 7205.
(60) Heinemann, C.; Koch, W.; Schwarz, H. *Chem. Phys. Lett.* **1995**, *245*, 509.
(61) Yao, C.; Guan, W.; Song, P.; Su, Z. M.; Feng, J. D.; Yan, L. K.; Wu, Z. *J. Theor. Chem. Acc.* **2007**, *117*, 115.

JP8024733